3F0496-02
Enclosure 7

Florida Power Corporation

ANALYSIS/CALCULATION SUMMARY

DOCUMENT IDENTIFICATION NUMBER	DISCIPLINE	CONTROL NO.	REVISION LEVEL
	M	96-0005	0

TITLE
MUT VORTEXING EVALUATION

CLASSIFICATION (CHECK ONE)
☒ Safety Related
☐ Non Safety Related

MAR/SP/CGWR/PEERE NUMBER

VENDOR DOCUMENT NUMBER

	REVISION APPROVALS		ITEMS REVISED
Design Engineer	David T. Wenkel		
Date			
Verification Engineer	P.L. Barko		
Date/Method*		R	
Supervisor			
Date			

***VERIFICATION METHODS:** R - Design Review; A - Alternate Calculation; T - Qualification Testing

DESCRIBE BELOW IF METHOD OF VERIFICATION WAS OTHER THAN DESIGN REVIEW

PURPOSE SUMMARY

The purpose of this calculation is to determine the submergence depth necessary in the MUT to prevent the entrainment of the overgas innto the outflow liquid.

RESULTS SUMMARY

The results of the analysis show that a submergence depth of 3.63 inches is required for a flow of 325 GPM out of the tank. Other submergence criteria are provided on page 4 of the calculation for different flow rates.

9604050448 960404
PDR ADOCK 05000302
P PDR

TABLE OF CONTENTS

ATTACHMENTS

1.0 Purpose:

The purpose of this calculation is to determine the submergence depth necessary in the MUT tank to prevent the entrainment of the tank's overgas in the outflow stream. This type of hydraulic abnormality can lead loss of pump efficiency, possible cavitation, vibration, surging, etc. and damage to the pump.

2.0 Design Inputs:

2.1 Buffalo Tank Dwg. M-6057
2.2 Attachments 1.0 & 2.0

3.0 Assumptions:

This analysis does not contain any assumptions requiring later confirmation or preliminary data.

4.0 References:

4.1 Weak Vortices at Vertical Intakes, *Journal of Hydraulic Engineering*, Vol. 113, No. 9, Sept., 1987 (see Attachment 1)
4.2 Sizing Piping for Process Plants, Chemical Engineering, June 17, 1968, pages 205 & 206 (see Attachment 2)

5.0 Calculation:

Reference 4.1 gives the results of studies of weak vortices in intake structures that have vertical outlets that convey the water to the pump suction. This paper develops an equation that can be used to estimate if weak vortices can form on the free surface of the water in the intake. This configuration is very similar to the free water surface within the MUT tank.

However, the tank does not have the mechanism within the internal flow path of the tank to mechanically induce circulation flow. All water inputs to the tank are directed to the surface by spray nozzles. There are no side entrances which would allow a tangential flow velocity to develop to create a circulation flow around the suction nozzle at the bottom of the tank.

Therefore, the equation developed in the reference 4.1 can be used to estimate the submergence necessary to preclude the formation of weak surface vortices which may damage the pump by allowing the tank's overgas to be entrained in the outflowing liquid.

The equation from reference 4.1 is

$$S/D = 2.5 + [\ 4/3\ ]\{\ F_D\ \}^{(2/3)} + 40\ \{\ N_\Gamma\ \}^{0.3}$$

where: S is the submergence, inches
D is the diameter of the outflow pipe, inches
F_D is the Froude No. based on velocity in and diameter of the outflow pipe, $V/(gD)^{0.5}$
N_Γ is the circulation number

For the MUT tank, the circulation number is zero. Therefore, this equation reduces to the following

$$S/D = 2.5 + [\ 4/3\ ]\{\ F_D\ \}^{(2/3)}$$

The required submergence can be evaluated for various outflow rates in GPM. The results of this evaluation are given below.

GPM	Velocity, ft/sec	Froude No.	Submergence, in
25.0	0.63	0.192	11.85
50.0	1.26	0.384	12.9
75.0	1.89	0.575	13.78
100.0	2.52	0.767	14.56
125.0	3.15	0.957	15.29
150.0	3.78	1.151	15.96
175.0	4.41	1.343	16.6
200.0	5.04	1.534	17.2
225.0	5.67	1.726	17.79
250.0	6.3	1.918	18.35
275.0	6.93	2.11	18.9
300.0	7.56	2.302	19.42
325.0	8.19	2.493	19.94
350.0	8.82	2.685	20.43

Reference 4.2 has information on the flow conditions that will develop inside the tank near the exit point when the liquid level is approaching the pipe exit or the bottom of the tank. These flow conditions are has follows. A liquid circular weir will form when the Froude number is less than roughly 0.3 or the ratio of submergence height to diameter of the outlet pipe is less than 0.25. With this flow configuration, the vapor/gas core that is formed in the pipe and tank is not appreciably pulled into the downflowing liquid. For this flow condition, the flow is self venting.

When the Froude number is greater than 0.3, vapor/gas will be entrained into the downflowing liquid unless sufficient liquid height is maintained in the tank. This entrainment height can be evaluated by Harleman's equation presented in reference 4.2. This equation is presented below.

$$S/D = [\ V/(\ 3.24\ \{gD/12\}^{0.5})]$$

Where: S is the submergence, inches
D is the diameter of the outflow pipe, inches
V is the velocity of the liquid in the outflow pipe, ft/sec
g is 32.174 ft/sec^2

Using this equation, the following table presents the submergence to prevent gas entrainment vs. outflow rates in gpm.

GPM	Velocity, ft/sec	Froude No.	Submergence,in
25	0.63	0.192	1.3
50	1.26	0.384	1.72
75	1.89	0.575	2.02
100	2.52	0.767	2.65
125	3.15	0.957	2.48
150	3.78	1.151	2.66
175	4.41	1.343	2.83
200	5.04	1.534	2.99
225	5.67	1.726	3.13
250	6.3	1.918	3.27
275	6.93	2.11	3.39
300	7.56	2.302	3.52
325	8.19	2.493	3.63

6.0 Results:

The submergence given by the equation of reference 4.2 is considered the proper method to evaluate for gas/vapor entrainment into the downflowing liquid exiting from the MUT into its outflow pipe. The results of the reference 4.1 equation are not considered viable since the tank configuration and flow conditions into the tank are not the same as those used in the reference 4.1 to develop the equation.

ANALYSIS/CALCULATION
DOC ID # ~~M94-0053~~ M96-0005 ATT # ~~XX~~ 1
REV 20 SHEET 1 OF 12

WEAK VORTICES AT VERTICAL INTAKES

By John S. Gulliver,[1] M. ASCE, and Alan J. Rindels[2]

ABSTRACT: Weak, free surface vortices at vertical intakes with a headrace channel are defined by the first observence of a persistent dye core upon dye injection. Dimensionless parameters describing free surface vortex flows are used in an analysis of experimental data. The experimental results indicate that a large dimensionless submergence is required to avoid weak vortices at vertical intakes. Most vertical intakes will therefore require some type of antivortex device if weak vortices are to be avoided. The required dimensionless submergence is also highly dependent upon approach flow angle and headrace length/width ratio.

INTRODUCTION

Intake vortices are a result of angular momentum conservation at the flow constriction where angular velocity increases with the decrease in cross-sectional area. They occur commonly at free surface flows into closed conduits, such as sinks or bathtub drains. In large closed conduit intakes, however, vortices are often a severe problem to be avoided. They have been found to cause flow reductions, vibrations, structural damage, surging due to vortex formation and dissipation, and a loss of efficiency in turbines or pumps. In certain instances they have also been a safety hazard.

Pump and turbine performance is highly sensitive to swirling flow. Hydraulic pumps and turbines are designed assuming that the flow into the machine will be axial and uniform. An intake vortex can cause a swirling flow to enter the machine, resulting in off-design operation, a loss of efficiency, and possibly cavitation, surging, and vibration. An air-entraining vortex can also reduce the discharge into the intake. Sweeney, et al. (1982) state that at pump intakes no organized or subsurface vortices equal to or greater than that visually represented by a coherent swirl into the intake (dye core vortices) can be allowed. Trash-pulling and air core vortices, therefore, should also be avoided. A similar criterion is appropriate for hydroturbine intakes, since the flow through the hydromachine is similar. One difference from a pump, however, is that a turbine has guide vanes upstream of the runner that may eliminate a small swirl. Another difference is that wall friction in a long penstock may eliminate swirl before it reaches the turbine (Baker and Sayre 1974; Hecker and Larson 1983).

This paper presents the results of an experimental investigation designed to predict the formation of weak, free-surface vortices at vertical intakes with a headrace channel. A weak vortex is defined as a coherent.

[1]Assoc. Prof., St. Anthony Falls Hydr. Lab., Dept. of Civ. and Mineral Engrg., Univ. of Minnesota, Minneapolis, MN 55414.
[2]Grad. Res. Asst., St. Anthony Falls Hydr. Lab., Dept. of Civ. and Mineral Engrg., Univ. of Minnesota, Minneapolis, MN 55414.

Note.—Discussion open until February 1, 1988. To extend the closing date one month, a written request must be filed with the ASCE Manager of Journals. The manuscript for this paper was submitted for review and possible publication on February 18, 1986. This paper is part of the *Journal of Hydraulic Engineering*, Vol. 113, No. 9, September, 1987. ©ASCE, ISSN 0733-9429/87/0009-1101/$01.00. Paper No. 21775.

ent dye core entering the intake, a class of vortices to be avoided np and turbine intakes. The primary application of the results is preliminary design of vertically arranged intakes for hydropower es. The experiments emphasize approach flow angle, intake subnce, intake velocity, and the length/width ratio of the headrace.

…eters Influencing Vortex Formation

flow field in which intake vortices occur is highly three-dimenl, allowing only minimal simplification of the equations of motion. dimensionless parameters that should be used to describe vortex ation have been in debate for two decades, one example being the of Jain, et al. (1978), and following discussions (Amphlett 1979; dell 1979; Hebaus 1979). Recently, Odgaard (1986) has used a Ranvortex and an assumption on the definition of an air-entraining voro theoretically develop an equation for the submergence required oid such a vortex. The applicability of Odgaard's work, especially ye core vortices, has not been tested, however.

e most desirable dimensional analysis involves normalization of the ations of motion, as was performed by Anwar (1966). The authors repeated Anwar's analysis, resulting in a slightly different set of ensionless parameters. The equations of motion for a steady incomsible flow with axial symmetry (Fig. 1) may be expressed in terms he dimensionless stream function, ψ, first defined by Lewellen (1962)

$$\frac{Q}{r}\frac{\partial\psi}{\partial z} \qquad (1a)$$

$$v_z = -\frac{Q}{r}\frac{\partial\psi}{\partial r} \qquad (1b)$$

d the dimensionless variables $\eta = r/D$; $\zeta = z/S$; and $\Gamma = 2\pi(v_\theta r/\Gamma_\infty)$ give

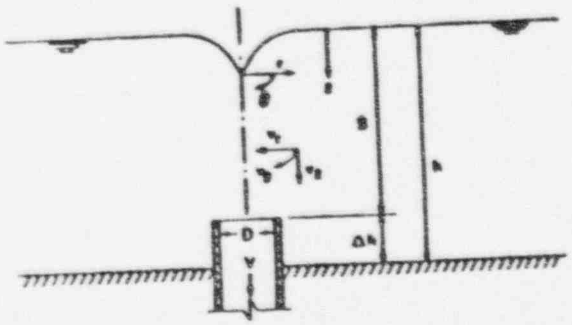

FIG. 1.—Definition Sketch for Variables and Parameters of Vortex Formation at Vertical Intake

ANALYSIS/CALCULATION M96-0005
DCC ID # M4M-0005 ATT # A1
REV 0 SHEET 2 OF 7

$$\eta\frac{\partial\psi}{\partial\zeta}\frac{\partial^2\psi}{\partial\eta\partial\zeta} - \left(\frac{\partial\psi}{\partial\zeta}\right)^2 - \eta\frac{\partial\psi}{\partial\eta}\frac{\partial^2\psi}{\partial\zeta^2} = \left(\frac{S\Gamma_\infty}{Q}\right)^2\frac{\Gamma^2}{4\pi^2}$$

$$-\frac{r^3}{\rho}\frac{\partial P}{\partial r}\frac{S^3}{Q^2} + \frac{\nu S}{Q}\left[\eta^2\frac{\partial^3\psi}{\partial\eta^2\partial\zeta} - \frac{\partial^2\psi}{\partial\eta\partial\zeta} + \left(\frac{D}{S}\right)^2\eta^2\frac{\partial^3\psi}{\partial\zeta^3}\right] \qquad (2)$$

$$\frac{\partial\psi}{\partial\zeta}\frac{\partial\Gamma}{\partial\eta} - \frac{\partial\psi}{\partial\eta}\frac{\partial\Gamma}{\partial\zeta} = \frac{\nu S}{Q}\left[\eta\frac{\partial^2\Gamma}{\partial\eta^2} - \frac{\partial\Gamma}{\partial\eta} + \left(\frac{D}{S}\right)^2\eta\frac{\partial^2\Gamma}{\partial\zeta^2}\right] \qquad (3)$$

$$\frac{1}{\eta^3}\frac{\partial\psi}{\partial\zeta}\frac{\partial\psi}{\partial\eta} - \frac{1}{\eta^2}\frac{\partial\psi}{\partial\zeta}\frac{\partial^2\psi}{\partial\eta^2} + \frac{1}{\eta^2}\frac{\partial\psi}{\partial\eta}\frac{\partial^2\psi}{\partial\eta\partial\zeta} = \left(g - \frac{1}{\rho}\frac{\partial P}{\partial z}\right)\frac{SD^4}{Q^2}$$

$$+\frac{\nu S}{Q}\left[-\frac{1}{\eta}\frac{\partial^3\psi}{\partial\eta^3} + \frac{1}{\eta^2}\frac{\partial^2\psi}{\partial\eta^2} - \frac{1}{\eta^3}\frac{\partial\psi}{\partial\eta} - \left(\frac{D}{S}\right)^2\frac{1}{\eta}\frac{\partial^3\psi}{\partial\eta\partial\zeta^2}\right] \qquad (4)$$

where v_r, v_z, and v_θ = the radial, axial, and angular velocity components, respectively; r, z, and θ = the radial, axial, and angular coordinates; P = pressure; ρ = fluid density; g = the acceleration of gravity; ν = kinematic viscosity of the fluid; S = submergence; D = intake throat diameter; Q = flow rate; and Γ_∞ = the farfield values of $2\pi\, v_\theta r$ (circulation). Using S, rather than D, in the expression for ζ results in a relatively simple dimensionless expression for circulation, as will be shown later. Eqs. 2, 3, and 4 identify six dimensionless parameters which describe the flow: $N_\Gamma = S\Gamma_\infty/Q$, a circulation number; $R = Q/\nu S$, a Reynolds number; S/D, a dimensionless submergence; $(r^3/\rho)(\partial P/\partial r)(S^3/Q^2)$; $(1/\rho)(\partial P/\partial z)(SD^4/Q^2)$; and gSD^4/Q^2. (The latter three parameters will be converted to dimensionless variables in Eqs. 9 and 10.) Dividing Eq. 2 by $(S/D)^2$ would isolate the circulation number identified by Anwar (1966), $D\Gamma_\infty/Q$. This is at first appearance a more logical choice than $N_\Gamma = S\Gamma_\infty/Q$, since the submergence, which is frequently a dependent parameter, is replaced by the intake diameter. The ratios Γ_∞/Q, however, may be reduced to a form that is inversely dependent upon submergence, resulting in a very simple relationship for N_Γ as defined herein.

Consider the sketch of a vertical intake shown in Figs. 1 and 2. The far-field circulation is the line integral of angular velocity times radius at $r = R$:

$$\Gamma_\infty = \int_0^{2\pi} R v_\theta d\theta = 2\pi v_\theta R = 2\pi R v_r \tan\alpha \qquad (5)$$

where α = the angle between the approach velocity vector $\vec{V}$ and the vector normal to the control surface. In addition, the discharge through the cylindrical control surface of radius R and height $S + \Delta h$ is

$$Q = 2\pi R v_r(S + \Delta h) \qquad (6)$$

Then, our dimensionless circulation parameter becomes

$$\frac{S\Gamma_\infty}{Q} = \frac{2\pi v_r RS\tan\alpha}{2\pi R v_r(S + \Delta h)} = \frac{\tan\alpha}{\left(1 + \dfrac{\Delta h}{S}\right)} \qquad (7)$$

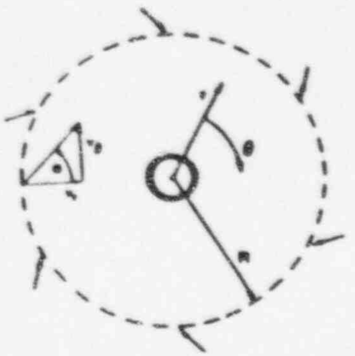

—Plan Sketch of Vertical Intake for Parameter and Variable Definition

/S is often small, the circulation parameter identified herein may, n cases, be expressed as

$$\frac{\tan\alpha}{1 + \frac{\Delta h}{S}} \approx \tan\alpha \quad \text{(8)}$$

ìrculation parameter given by Eq. 8 is similar to that used by al. (1978) in the analysis of their experimental data because it l in less auto-correlation between the independent parameters of ·gression; e.g., submergence was not incorporated into the cir- n parameter. The equations developed herein give a theoretical or this decision.

two pressure gradient terms resulting from Eqs. 2 and 4 will in- the Froude numbers that govern the intake vortex flow. If we e that the pressure distribution is approximately hydrostatic, then = ρg, and $\partial P/\partial r = \rho g \partial z/\partial r$, where z = the distance from the water . The pressure gradient and body force terms in Eq. 4 then be-

$$\left(\frac{1}{\rho}\frac{\partial P}{\partial z}\right)\frac{SD^4}{Q^2} = 0 \quad \text{(9)}$$

ng as the pressure distribution is close to hydrostatic in the vertical ion, which is a good assumption for weak vortices, the gravity and ure gradient terms in Eq. 4 cancel. In addition, the pressure gra- and body force terms in Eq. 2 become

$$\frac{S^2}{Q^2} = \frac{gS^3D^2}{Q^2}\eta^2\frac{\partial\zeta}{\partial\eta} = \frac{16}{\pi^2}\frac{\left(\frac{S}{D}\right)^2}{F^2}\eta^2\frac{\partial\zeta}{\partial\eta} = \frac{16}{\pi^2}\frac{\left(\frac{S}{D}\right)^3}{F_D^2}\eta^2\frac{\partial\zeta}{\partial\eta} \quad \text{(10)}$$

e $F = V/\sqrt{gS}$, $F_D = V/\sqrt{gD}$; and V = mean inlet velocity = $4Q/$. Eq. 10 indicates that the choice of a proper Froude number, given ìrculation parameters of Eq. 8, is not straightforward. The appro-

priate relationship between S/D and Froude number, however, can be seen from Eq. 10 to be $S/D \sim F$ or $S/D \sim F_D^{2/3}$. The writers' experience is that when measured values of S/D at which a given type of vortex occurs are plotted versus the Froude number, $F_D = V/\sqrt{gD}$, and a circulation parameter, $N_\Gamma = \tan\alpha$, a far better resolution of the data is achieved. A comparison of S/D versus $F = V/\sqrt{gS}$ and $\Gamma_\infty D/Q = D\tan\alpha/S$ could result in a cloudy resolution of the data because a dependent variable in the experiments, submergence, is contained in each of the three terms. Measurement errors in submergence would affect each of the three variables.

Reduction of Circulation along Headrace Channel

A number of researchers have experimentally investigated free surface vortex formation at an outlet in the center of a tank floor with a given circulation (Anwar 1966; Daggett and Keulegan 1974; Jain, et al. 1978). The circulation was controlled using vanes or using jets issuing from the side of the tank (Chang 1976). The typical vertically arranged hydroturbine intake structure, schematically shown in Fig. 3, is far from a circular tank, however. Although the approach flow circulation (angle) may be estimated, the effect of the structure near the intake on circulation is generally unknown and difficult to determine (Brochard 1983). Most hydroturbine intakes also have an approach channel (headrace) that will significantly reduce the circulation in the approach flow. N_Γ at the upstream end of the headrace will remain the same because Γ_∞ and Q are both reduced by the factor $B/(2\pi R)$, where B = the headrace width.

The primary reason a headrace will reduce circulation is the lateral difference in energy grade line $[h + V^2/(2g)]$ caused by the flow separation around the leading edge of the channel walls. Higher velocities and possibly even a higher water surface elevation will occur on the left wall (Fig. 3), looking toward the intake. The energy grade-line on the right wall will be less than that at the left wall, reducing the transverse flux of momentum. This reduction of circulation is a function only of intake geometry (L/B) and flow approach angle.

Circulation will be reduced further by side wall friction. The process is slow, however, requiring much larger L/B ratios than normally en-

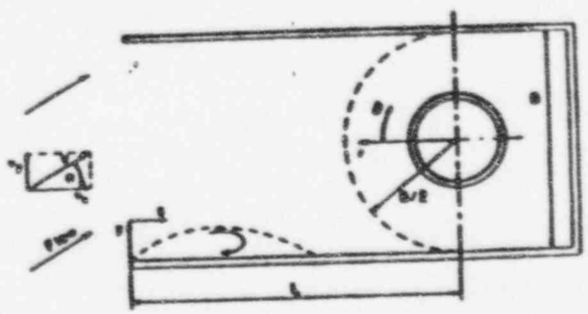

FIG. 3.—Definition Sketch of Vertical Intake with Headrace Channel

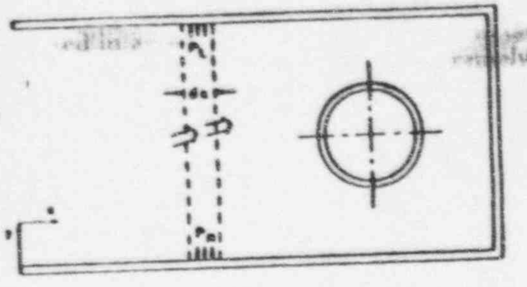

4.—Control Volume for Momentum Theorem Application

ı the field, since the wall boundary layer increases gradually ce. This phenomenon will be neglected here.

nts were performed on an intake very similar to that of Fig. to describe the reduction of circulation along the headrace number of dimensionless parameters using tan α, L/B, etc. without success. Finally, a very approximate momentum flux ıs developed that proved successful. If we assume: (1) That on in circulation is proportional to the reduction of the y- of momentum in the channel; (2) that the cross-sectional mean nt of velocity V_y may be used in the momentum theorem, 0, $V_y = V \tan\alpha$; and (3) that the pressure difference between l right walls is proportional to the y-component velocity head, (Fig. 4):

$$-\frac{1}{2}\beta\rho V_y^2 \qquad (11)$$

= pressure on the right wall; P_L = pressure on the left wall; ı constant of proportionality on the order of one or two, then ntum theorem may be integrated between $x = 0$ and $x = L$,

$$= \frac{S}{h}\tan\alpha \frac{1}{1 + \frac{\beta}{2}\frac{L}{B}\tan\alpha} \qquad (12)$$

$S + \Delta h$, and $S >> \Delta h$ in most applications, we will assign

$$\frac{\tan\alpha}{\frac{\beta}{2}\frac{L}{B}\tan\alpha} \qquad (13)$$

ill be used in an analysis of the experimental data presented in section. Assumptions 1 and 2 are an extremely gross approxi- f reality. The other option, however, is to attempt various com- s of the relevant numbers at random, which certainly would not duced the relation for N_f^* given in Eq. 13.

Experimental Facility

An experimental flume was built to investigate vortex formation in vertical intakes with a headrace channel. The flume, shown in Figs. 5 and 6, is 7 m (23 ft) long, 1.4 m (5 ft) wide, and 1.2 m (4 ft) deep, consisting of a stilling basin, a transition section, and a test section. Flow was supplied from the Mississippi River in a once-through mode with a 20-cm (8-in.) supply line to the stilling basin. Inflow was measured with an orifice meter calibrated in-line and connected to a manometer with either mercury or Meriam blue as indicator fluids. The stilling basin was designed to produce a fairly straight uniform flow out of this section. This was achieved with a 20-cm (8-in.) lateral diffuser pipe shown in Figs. 5 and 6 with 5 cm (2 in.) diameter holes drilled to stagger at +45° and −20° off horizontal, and directed at the rear wall. The flow was further smoothed by flowing through a 15-cm (6-in.) thick rock crib, which consisted of rocks coarser than a 2-cm (3/4-in.) sieve. Finally, a transition zone of 2 m (7 ft) was used to dampen any large scale eddies. Velocity measurements after the rock crib indicated a relatively uniform velocity over the cross section (Rindels and Gulliver 1983).

Visual observation was made possible by installation of two 1.2 m × 1.4 m × 2 cm (4 ft × 8 ft × 3/4 in.) plexiglass walls at the side and end

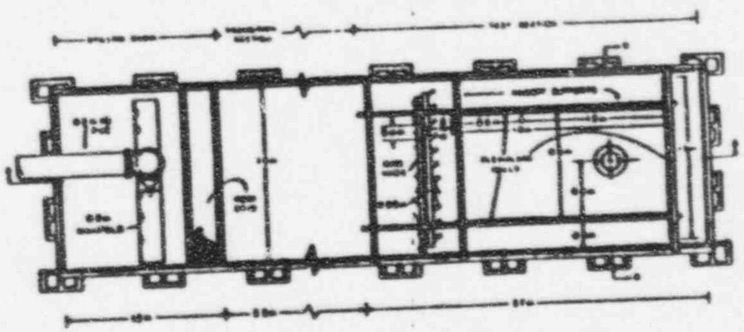

FIG. 5.—Plan View of Experimental Facility

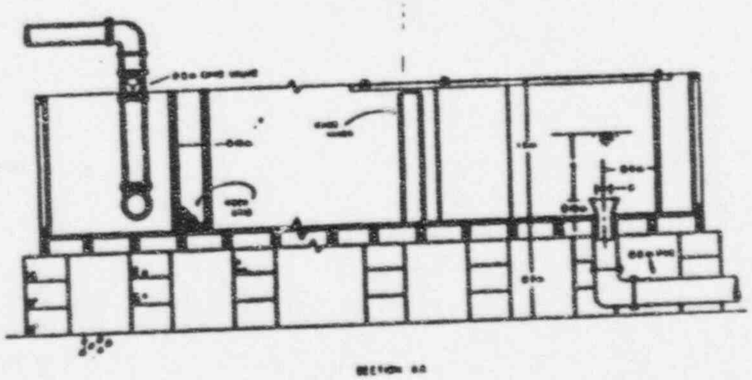

SECTION AA

FIG. 6.—Section View of Experimental Test Facility

lume. The interior components of the test section were the mov- adrace walls and the bellmouth intake. The variable length side- vere produced using four plexiglass panels for each wall, which ed large variations in length. The length of the headrace walls tc k wall used in the experiment were the 0.9-m (3-ft), 1.8-m (6-ft), 9-m (9.5-ft) long combinations. The 1.8-m (6-ft) combination is in Figs. 5 and 6. The bellmouth was centered 0.4 m (16 in.) from ir sidewalls as shown in Figs. 5 and 6.

rder to control and predetermine the flow approach angle to the ace, guide vanes were located 11 cm (4.5 in.) upstream of the mov- dewalls. The 11 vanes were 21 cm (9 in.) in length with a thickness cm (0.12 in.) and a spacing of 11 cm (4.5 in.). Each vane had pivots top and bottom in order to vary approach flow angle between . Using a technique described by Jain, et al. (1978), the vane angle hickness were used to compute the angle of the flow leaving the . The maximum adjustment for vane thickness in computing the of the flow was 2%. Guide vane performance was evaluated through ographs of dye streaklines taken at two depths and two values of e discharge (Rindles and Gulliver 1983). The streaklines indicated the guide vanes performed their function well and that guide vane e is a good representation of approach flow angle. There was no ence of vorticity in the flow caused by the vanes.

n intake throat diameter of 0.15 m (6 in.) was chosen to avoid vis- impedance of vortex formation except at very low intake velocities, ough there is still uncertainty on the criteria. The throat diameter eeded Jain, et al.'s (1978) criterion of $g^{1/2}D^{3/2}/\nu > 5 \times 10^4$. Dagget and ilegan's (1974) criterion of $R_D \geq VD/\nu \leq 3.2 \times 10^4$ to avoid viscous cts indicate that viscous impedance of vortex formation is possible $V \leq 0.2$ m/s (0.68 ft/sec) or at $F_D \leq 0.17$. This criterion is surpassed virtually all of the data taken. Anwar's (1978) criterion of $R = Q/(\nu S)$ $\times 10^4$ indicates that the ratio $(S/D)/F_D$ must be less than five to avoid cous effects at water temperatures near 20° C. Anwar's criterion is o surpassed by most of the data. Data presented in Tullis, et al. (1986) licate a criterion of $R \geq 4 \times 10^4$ and a throat diameter, $D \geq 5$ in., hich are also surpassed by the data presented herein. Padmanabhan id Hecker (1984) found no significant scale effects above $R = 1.5 \times 10^4$. ich of these criteria was developed for air-entraining vortices, with large locities near the air core. A similar criterion for weak vortices would gically be somewhat less restrictive. Tullis, et al. (1986), for example, ound no scale effects for dye core vortices down to an $R = Q/(\nu S)$ of pproximately 5,000.

Measurement Technique

The measurements were designed to identify the submergence at which coherent, persistent dye core vortex forms, herein called critical sub- nergence. A coherent dye core vortex present for at least ten sec was defined as persistent. Ten sec was believed to be sufficiently long to avoid the fleeting vortices that will pass through the flow field. The dye- core vortex was chosen because it is the type of vortex that should be avoided in most pump and turbine intake designs.

For a given experimental run, inflow discharge and water surface el- evation were continually monitored over time. Water surface elevation was also recorded on a strip chart. Discharge into the bellmouth intake was found by adding inflow discharge to the product of water surface time rate of change and water surface area. Water surface elevation was allowed to drop slowly until a persistent dye core vortex formed, as de- termined visually by injecting dye through a syringe into the water. Water surface rate of change varied between a negligible value and 2×10^{-3} m/s (0.6×10^{-3} ft/sec) with no discernible impact on the measured value of critical submergence for dye core vortices (Rindels and Gulliver 1983).

Other potential sources of experimental errors, aside from the water surface rate of change, were the approach flow angle, discharge mea- surements, and measurement of water/surface elevation. As stated pre- viously, it was documented that guide vane angle is a good represen- tation of approach flow angle, within 2%. Vane angle could be set to within ±0.5 degrees; thus, the uncertainty in the vane angle is ±7% at 7.5° and ±2% at 30°.

An orifice meter, calibrated in place, was used to measure discharge. The accuracy of the calibration is 0.5%. In addition, the discharge was unsteady for a number of reasons (Padmanabhan and Hecker 1984) in- cluding leakage, unsteady inflow, and the drop in water surface eleva- tion over time. Thus, the uncertainty in discharge measurement was ±0.006 cms (±0.21 cfs), corresponding to an uncertainty in Froude num- ber, $V/\sqrt{gD}$ of ±0.27. This is a significant source of error and could account for some of the scatter in the data.

There were three sources of error in the stage measurements (water surface elevation). The point gage used was accurate to ±0.6 mm (±0.002 ft). In addition, the wood in the flume would swell and contract in con- junction with successive periods of drying and wetting. This swelling and contraction caused the level of the top of the bellmouth to be slightly off, estimated to be ±0.3 mm (±0.001 ft). There was also a human error in measuring the water surface elevation, estimated to be ±1.2 mm (±0.004 ft). This caused the total uncertainty in measurement of stage to be less than ±1.4 mm (±0.005 ft), which corresponds to an error of ±0.01 in the dimensionless submergence.

The definition of a "persistent" dye core vortex is somewhat arbitrary and developed primarily for the convenience of the experiments. Hecker (1981) has suggested using the percent of time a vortex is present as a criteria for hydraulic model studies where turbine and pump intakes should have dye core vortices present less than 50% of the time. The writers found this criterion somewhat less arbitrary but difficult to in- corporate into the measurements reported herein.

The difficulty in identifying critical submergence stems from the fact that vortex formation is a transition phenomenon from a purely radial flow to a swirling flow. The point of transition is not well-defined be- cause there is a range of flow conditions over which either a purely ra- dial or a swirling flow can occur, similar to the well-known transition from laminar to turbulent boundary-layer flow. Just as a disturbance in the free stream over the boundary layer can cause a turbulent spot that later dissipates, a disturbance in the intake approach flow can cause a fleeting dye core vortex, which appears infrequently and will not signtly impact turbine or pump performance. This disturbance could ie, for example, to a temporary surge in the flow or a rare com- on of tip vortices shedding from part of the hydraulic structure. in any transition phenomenon, the results of the experiments will some scatter. Since the critical submergence is found by reducing ergence until a persistent vortex forms, measurement errors will a bias towards lower submergence levels. The conservative ap- h to submergence guidelines, therefore, is to place an envelope over the measured values of critical submergence, as suggested umphreys, et al. (1970).

LTS

e critical submergence at which persistent dye core vortices form measured over a range of intake Froude numbers from 0.25–2.2 at rangements of headrace aspect ratio and approach flow angle. In 91 individual measurements of critical submergence were made. The idual data are available as an addendum to Rindels and Gulliver). The distance between the intake and the side walls was always imes the throat diameter. The walls did not greatly impede swirl lopment over the intake. The data, therefore, should be seen as g a maximum value of submergence that will assure no dye core ces.

e measurements are plotted in Figs. 7, 8, and 9 as S/D versus F_D the thirteen combinations of approach angle and aspect ratio. All

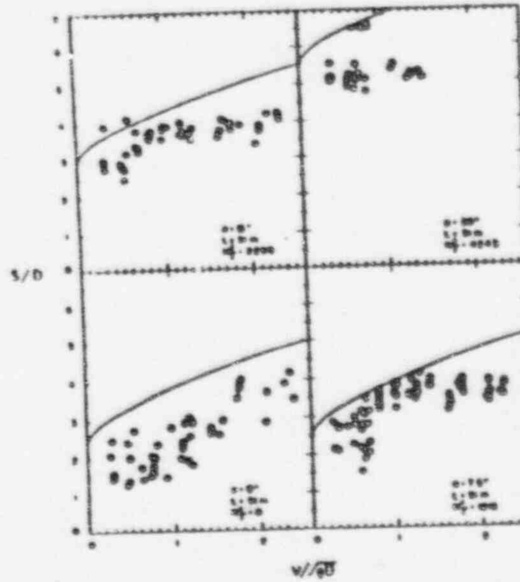

. 7.—Critical Submergence Measurements and Envelope Curves of Eq. 13 for adrace Length of 0.51 m (from Entrance to Intake Center Line); L/B = 0.63; = N?

DOC ID # ATT # REV R2 SHEET 6 OF

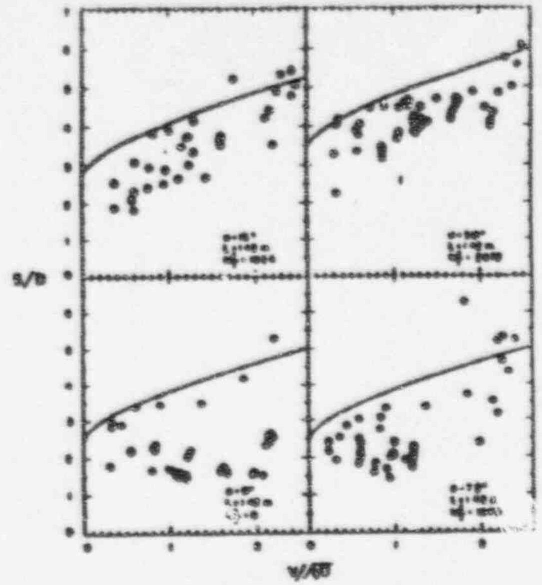

FIG. 8.—Critical Submergence Measurements and Envelope Curves of Eq. 13 for Headrace Length of 1.42 m; L/B = 1.75; N; = N?

measurements were made with an intake throat diameter of 0.15 m (0.5 ft) and a headrace width of 0.81 m (2-2/3 ft). The following observations may be made:

1. All of the arrangements required a significant dimensionless submergence to avoid dye core vortices, greater than 2.5.
2. Fig. 7 shows the critical submergence at the shortest headrace length, with L/B = 0.63. A great increase in the required submergence was apparent as the inflow angle changed from 15–30°. These short headrace and approach flow angles are similar to those of many hydropower facilities. Approach flow angle is thus an important parameter for these intakes..
3. The increase with approach flow angle is not as significant for an L/B ratio of 1.75, shown in Fig. 8, where an increase in α from 15–30° resulted in a relatively small (~ 0.7) increase in required S/D.
4. This increase in S/D with approach flow angle is reduced further with the relatively large L/B ratio of 3.14. In fact, even the extreme flow approach angle of 60° increased the required dimensionless submergence by only 0.8.
5. The required submergence for α = 60° and L/B = 3.14 is approximately the same as for α = 30° and L/B = 1.75. Thus, the effect of the headrace length/width ratio upon reducing circulation is obvious.
6. The data are all roughly the same for the three length/width ratios when $\alpha \leq 15°$. This indicates that the approach angle into the channel may not be of importance if it is less than 15°.

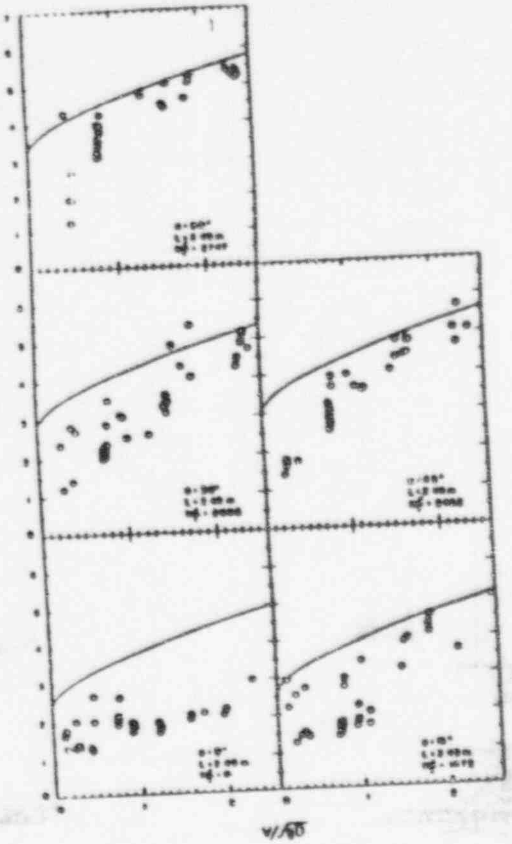

9.—Critical Submergence Measurements and Envelope Curves of Eq. 13 for ...race Length of 2.49 m; $L/B = 3.14$; $N_\Gamma^* = N_\Gamma^*$

...lso plotted in Figs. 7, 8, and 9 is a best-fit envelope curve developed ...onsidering all of the data simultaneously in linear regressions on ...14, successively changing the power on the N_Γ^* term, and attempting ...e values of β (β = 1, 2, and 3). The regression weighted the squared residuals be...duals above the envelope curve ten times the squared residuals ...the envelope curve. The resulting equation is as follows:

$$... 2.5 + \frac{4}{3} F_D^{2/3} + 40\, N_\Gamma^{*3} \quad \text{(14)}$$

...ere $F_D = V/\sqrt{gD}$; V = velocity in the intake throat; N_Γ^* = ...$\alpha/[1 + (L/B)\tan\alpha]$, (i.e., β = 2); and L = distance from the headrace ...rance to intake center line.

...hese equations are applicable for $0.2 \le F_D \le 2.5$. The $F_D^{2/3}$ dependence ...hat developed in Eq. 10. The ability of Eq. 14 to describe a range of ...nfigurations indicates that the approximate momentum theorem anal-

CALC ID + M96-0003 ATT # 1
REV 0 SHEET 7 OF 12

ysis with β = 2 gave acceptable results. These results will give an indication of the maximum submergence required to avoid dye core vortices at an intake with a headrace channel. A manually produced flow net (Gulliver, et al. 1986) may often be used to determine the angle of the approach flow to the intake. Positioning the side walls closer to the intake and the installation of antivortex devices will reduce the required submergence significantly. Presently, a hydraulic model study is the best (and perhaps the only) means of incorporating the various arrangements into the intake design.

Eq. 14 is most comparable to the results of Jain, et al. (1978), who measured the submergence at which an air-entraining vortex would form at a vertical intake. Jain, et al. found that the relation:

$$\frac{S}{D} = 5.6 N_\Gamma^{*0.42} F_D^{0.50} \quad \text{(15)}$$

gave a good description of their data when viscous effects were excluded. The primary differences between Eq. 15 and those developed herein is that Eq. 14 has an intercept at $S/D = 2.5$ and a much stronger dependence upon N_Γ^*. Both differences are probably due to the opposing criteria for critical submergence, e.g., dye core versus air-entraining vortices. Dye core vortices are chosen as a criterion herein because they should be avoided in most turbine and pump intakes (Sweeney, et al. 1982).

Example Application

The Rapidan hydroplant is a retrofit of an existing dam, with two 2.5-MW turbines, half the number originally installed with a greater total capacity. Intake vortices were one of a number of concerns with this retrofit. The following data apply: S = 24.5 ft (7.47 m); D = 9.75 ft (2.97 m); Q = 620 cu ft/sec (17.6 m^3/s); V = 8.3 ft/sec (2.53 m/s); $L/B = 1.33$; $F_D = 0.47$; and $S/D = 2.5$.

An electric analog potential flow analysis was carried out on the intake (Gulliver, et al. 1986) and could be used to determine the angle of approach flow. The five streamlines flowing into the right headrace were at the following angles (one headrace width away from the entrance): 40°, 52°, 65°, 90°, and 90°. These are very poor approach conditions. The average of these streamline angles, 67°, was used in determining that $N_\Gamma^* = 0.57$. Eq. 14 indicates that with these conditions an S/D value of 10.7 would be required to avoid free surface vortices. The intake was very close to the headrace walls, and the required submergence is probably less, but this gives an indication that a hydraulic model study is necessary, even with an S/D of 2.5.

The hydraulic model study that was commissioned confirmed that there was a vortex problem at the intake. A strong air core vortex formed that was difficult to eliminate, primarily because of the poor approach of the flow to the headrace (Gulliver, et al. 1986).

Summary and Conclusions

Weak, free surface vortices, defined by a coherent, persistent dye core subsequent to dye injection, have been studied for vertical intakes with

Ref 4-2 · Pg 1 of 2

considered to be the best experimental result; it is $V_B = 0.35\,(g_L D)^{1/2}$. These results agree with those for a downflowing liquid around a stationary bubble.

In summary, large ($d \geqq 1$ in.) long bubbles become trapped in vertically downflowing liquids when $\mu <$ 100 cp. and:

$$V_L = 0.31\sqrt{g_L D} \qquad (16)$$

When the velocity is less than predicted by Eq. (16), bubbles will rise. And at higher velocities, bubbles will be swept downward and removed from the pipe. If a continuous source of vapor is available, $0.31 \leqq V_L/(g_L D)^{1/2} < 1$ can be expected to produce pressure pulsation and vibration.

Fig. 12 has been prepared to aid in the solution of Eq. (16). The flowrate is converted to gpm., the diameter is changed to in., and ρ_G is assumed to be much less than ρ_L. Two additional lines are plotted on Fig. 12. The first is for $(N_{Fr})_L = 1$, near which pressure pulsation amplitudes will be high and siphons will form readily. The second line is encountered when $(N_{Fr})_L$ is increased further; frictional force offsets gravitational force, and no pressure gradient will be present in vertical downflow. This latter line depends on the Reynolds number and pipe roughness. The line given is for high turbulence conditions (e.g., water) with $\epsilon = 0.00015$ ft.

Irrotational Downflow From Process Vessels

Irrotational downflow is often confused with the large-bubble phenomenon inside a vertical pipe. Flow patterns at the exit of a process vessel, however, are more complex than the simple bubble dynamics. Liquid height and entrance geometry become important variables that complicate the analysis.

With the geometry shown in Fig. 13, liquid forms a circular weir in the vessel when the Froude number $V_L/(g_L D)^{1/2}$ is less than roughly 0.3 or H/D is less than 0.25. Liquid flows down the pipe in a falling film. The center of the pipe and vessel contains a vapor core that is not appreciably sucked into the downflowing liquid. This self-venting flow is not completely predictable and, as a result, may occur at Froude numbers somewhat greater than 0.3. D. S. Ullock,[16] for example, indicated that the transition occurs at $(N_{Fr})_L = 0.55$.

When the Froude number exceeds 0.3, vapor will be entrained into the downflowing liquid unless sufficient liquid height is maintained in the process vessel. The entrainment point or critical liquid height has been determined experimentally by Kalinske,[22] and theoretically by Harleman and others.[23] Harleman's equation, shown in Fig. 13, should be a conservative design basis; vapor will not be sucked into the downpipe at or above the liquid height predicted by this equation.

The critical liquid height at which entrainment first occurs is frequently unknown. To test for vapor entrainment, the critical height is compared with that which would exist if entrainment were ignored. If the critical height is greater, vapor will be sucked into the downflowing liquid.

Harleman studied selective withdrawal of saline water solutions. It seems likely that his equation could also be applied to two immiscible liquid phases (decanter design). However, the coefficient of 3.24 given in Fig. 13 should be changed to his experimental value of 2.0. In addition, the lighter phase density should replace ρ_G in Eq. (14).

Whirlpools in Process Vessels

Compared with irrotational flow, whirlpool formation is usually very unpredictable because the forces

History of a Downflow Problem

Although the problems with downflow are many and varied, one particular problem is interesting because it illustrates a recurring design problem.

The piping configuration shown in the photograph was sized without any downflow technology. The 30-in. cooling-water return line, roughly 40 ft. long, was designed for approximately 13,000 gpm. of water. Bottom of the 30-in. line was near atmospheric pressure.

After startup, the equipment near this large water line vibrated severely. A study revealed that vibration originated in the 30-in. pipe. Furthermore, the pressure at the top of the pipe was near one psia. Also water temperature of 40 C. was uncomfortably close to the 39 C. boiling point of water at one psia. Thus, the continuous vapor source needed for pressure pulsation and vibration was apparently coming from water cavitation.

In hindsight, had Fig. 12 been available at the time, the designer could have predicted the siphon in the design stage, and made an appropriate change to eliminate the possibility of pressure pulsation. The line could have been made larger so that it was not liquid filled, or smaller so that friction would raise the pressure at the top of the pipe. The problem could also have been corrected with a restriction orifice near the base of the 30-in. line.

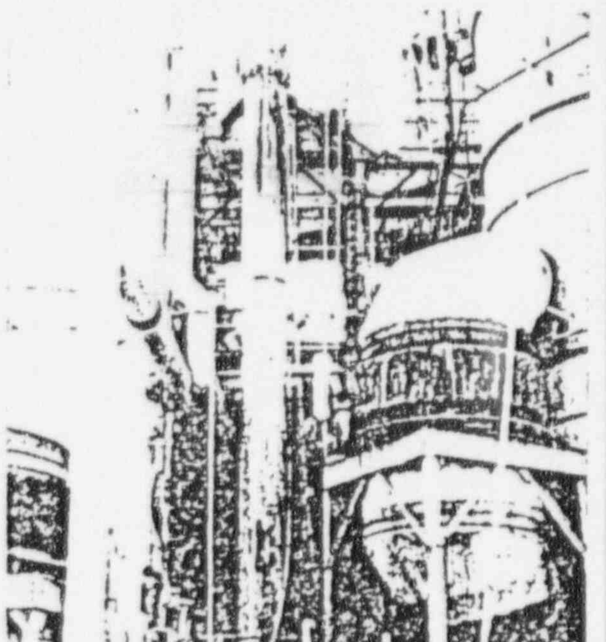

Pg 2 of 2

that initiate whirlpools are generally weak. Yet the effect of a whirlpool can be dramatic. The rotating liquid can open a vapor core in a vessel that will propagate through the outlet piping, and perhaps into a pump.

Although tangential inlets most easily initiate whirlpools, centrifugal pumps can also induce a rotating flow[24] in an upstream vessel that in turn opens a vapor core and feeds vapor into the pump suction. Whatever the cause, whirlpools can be easily eliminated with a straightening cross that is installed at the vessel outlet nozzle.

Two-Phase Upflow

Sizing of piping is particularly difficult with vapor and liquid in cocurrent upflow. If a line is sized for low pressure drop, it may well cause slug flow, with resultant pressure pulsation and vibration. A primary design objective must, therefore, be to avoid a slug-flow pattern.

At least four distinct flow patterns can be observed in upflow. In order of increasing vapor rate, these are: bubble, slug, froth, and annular. Only the slug-to-froth transition is of interest here.

Govier and others[25, 26, 27] have run extensive tests on vertical upflow of air-water mixtures. They experimented with tube diameters from 0.62 to 2.5 in. One series of tests studied the effect of liquid rate on flow patterns, while a second series concerned the effect of variation in vapor density on flow patterns.

In the slug-to-froth transition, we can study the flow pattern in terms of the Froude numbers $(N_{Fr})_L$ and $(N_{Fr})_G$. Such a correlation is shown in Fig. 14.

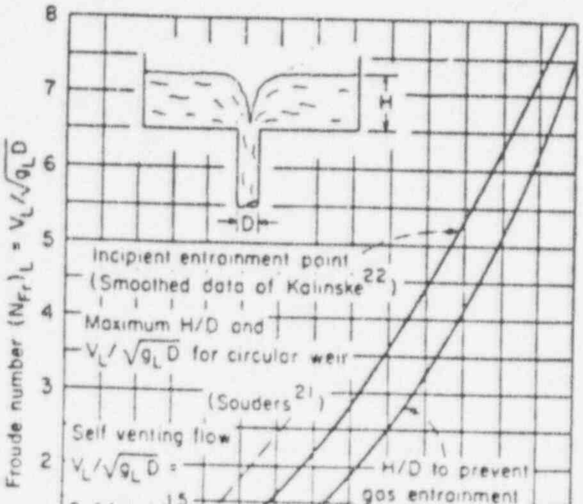

IRROTATIONAL downflow may occur in vessels—Fig. 13

The shaded area in this figure indicates uncertainty in the transition point. Actually, the uncertainty is much greater because the observation as to what constitutes froth or slug flow is somewhat arbitrary. The reader is referred to Govier's first article[25] for his distinction between slug and froth patterns.

Case History: Vibration From Upflow

One application of Fig. 14 involved vibration in a long 30-in. pipe in which two phases were flowing. A vertical riser at the end of the horizontal section vibrated at a low frequency and an intolerably high amplitude.

Three modifications were made to eliminate the suspected slug-flow pattern. The first change was a reduction in pipe size from 30-in. to 24-in. Only the riser and some horizontal piping immediately upstream of the riser were reduced. The second modification was to install more gradual horizontal-to-vertical transition piping. Finally, connections were installed for a vapor injection into the 24-in. transition piping. The injection nozzles were sized to supply momentum that was thought to be lost by the liquid at the transition. This last change was later found to be unnecessary.

When the new installation was placed in service, it was found to pass a higher vapor rate than before without appreciable vibration. As shown by the points in Fig. 14, the suspected flow patterns were predicted correctly.

Isothermal Two-Phase Pressure Drop

As with other aspects of two-phase flow, pressure-drop estimates have a high uncertainty associated with them. The designer should expect his pressure-drop estimate to be typically ±40% of the true value. Because of this uncertainty, he should try at least two different pressure-drop correlations if he desires additional confidence in his estimates.

Ideally, pressure-drop correlations should probably be specific for a particular flow regime. The reason is that a dispersed-flow pattern, for example, would be expected to behave different from a slug-flow pattern. This approach has not met with great success, partly because the available flow-pattern maps are not yet well defined.

Some correlations, notably that of Martinelli,[28] have failed to differentiate between frictional pressure drop and momentum-based pressure drop. This latter pressure drop is that associated with expansion of the gas phase as pressure is reduced. It is particularly important with the high mass velocities and the low pressures that are used to generate data for correlations.

Two correlations that will be considered here are the correlation of Lockhart and Martinelli,[28] and the homogeneous model of Dukler and others.[29] These correlations are easy to use, and are more accurate than most other correlations.[29, 30] Of the two, Dukler's correlation will be slightly better for most applications.

Both Martinelli's and Dukler's correlations can be expected to give better accuracy for horizontal flow